PERIODICA POLYTECHNICA SER. TRANSP. ENG. VOL. 24, NO. 1, PP. 29–46 (1996)

CHANGES IN GAS TURBINE MAPS AS RESULTS OF DIVERGENCE IN GEOMETRICAL PARAMETERS

Imre SÁNTA

Department of Aircraft and Ships
Technical University of Budapest
H–1521 Budapest, Hungary

Received: November 7, 1994

Abstract

The behaviour of the turbines of gas turbine power plants determines decisively the operation of the whole unit. Therefore, the detailed knowledge of it will be required, as well as the determinability of the changes in the operational characteristics as a function of geometrical and other parameters (damage). In this paper, the effect of the change in the geometrical parameters on the turbine characteristics is examined. The method of examination is based on the application of the mathematical model of the turbine. In the paper, the method of the mathematical description of the thermal hydraulic processes at the level of the row of blades, the equations incorporated in the model and the flow-chart of the algorithm for the mathematical model are described. The modification of the characteristics due to the change of the blade angles and the radial clearances is also demonstrated in it.

Keywords: gas turbine modelling, turbine map, losses, efficiency, multistage turbines, row of blades.

Nomenclature

c	–	absolute velocity
w	–	relative velocity, work
u	–	peripheral velocity
T	–	absolute temperature
p	–	absolute pressure
π	–	pressure ratio
n	–	number of revolution
f	–	fuel-to-air ratio
α	–	angle of absolute velocity
β	–	angle of relative velocity
i	–	enthalpy
c_p	–	mass specific heat at constant pressure
κ	–	adiabatic exponent
R	–	specific gas constant
A	–	area
λ	–	non-dimensional velocity

$\pi(\lambda)$ – pressure gas dynamic function
$\tau(\lambda)$ – temperature gas dynamic function
$q(\lambda)$ – non-dimensional mass flow rate
ρ – density
m – mass flow rate
Re – Reynolds number
ξ – loss coefficient
M – Mach number
η – efficiency
P – power
ψ – velocity-loss factor
l – chord of the blade
t – pitch
δ – radial clearance
h – height of the blade

Subscripts

1 – parameter at the inlet of the row of blades
2 – parameter at the exit of the row of blades
j – serial number of the row of blades
T – turbine
cr – critical
w – parameter in relative motion
0 – parameter at the throat
p – profile
t – theoretical (ideal)
u – tangential component
st – stage
fr – friction
te – trailing edge
cl – clearance
m – mean
$cool$ – cooling
mix – mixing
Re – parameter due to Reynolds number
s – isentropic

Superscripts

$*$ – stagnation parameter
$''$ – parameter at the tip diameter
$'$ – parameter at the root diameter

1. Turbine Modelling

Turbine model describes the processes occurring in the rows of blades by aero-thermodynamic equations and determines the exit parameters as function of inlet ones.

The turbine mathematical model is a method of calculation of the turbine map.

1.1. Calculation of the Row of Blade Parameters

The basic equations of calculations were developed from expressions of [1],[2].

Minimum cross-sectional area between blades

$$A_{0,j} = D_{2,j} h_j \pi \sin \beta_{2,j} \, . \tag{1}$$

Parameters of gas at the inlet

Data of velocity triangles

$$w_{1,h} = \sqrt{c_{1,j}^2 + U_{1,j}^2 - 2c_{1,j} u_{1,j} \cos \alpha_{1,j}} \, , \tag{2.a}$$

$$\beta_{1,j} = \tan^{-1} \frac{c_{1,j} \sin \alpha_{1,j}}{c_{1,j} \cos \alpha_{1,j} - u_{1,j}} \, . \tag{2.b}$$

Stagnation enthalpies in absolute and relative motion

$$i_{1,j}^* = c_p T_{1,j}^* \, , \tag{3}$$

$$i_{w1,j}^* = i_{1,j}^* - \frac{w_{1,j}^2 - c_{1,j}^2}{2} \, . \tag{4}$$

Stagnation temperature in relative motion at the inlet

$$T_{w1,j}^* = \frac{i_{w1,j}^*}{c_p} \, . \tag{5}$$

Gas dynamic functions

$$\lambda = \frac{c}{c_{cr}} \, , \quad \tau(\lambda) = \frac{T}{T^*} = 1 - \frac{\kappa - 1}{\kappa + 1} \lambda^2 \, , \quad \pi(\lambda) = \frac{p}{p^*} = \tau(\lambda)^{\frac{\kappa}{\kappa - 1}} \, ,$$

$$q(\lambda) = \frac{\rho c}{\rho_{cr} c_{cr}} = \lambda \left[\tau(\lambda) \frac{\kappa + 1}{2} \right]^{\frac{1}{\kappa - 1}} \, . \tag{6}$$

From what

$$\lambda = \left\{ \left[1 - \pi(\lambda)^{\frac{\kappa-1}{\kappa}} \right] \frac{\kappa+1}{\kappa-1} \right\}^{\frac{1}{2}} . \tag{7}$$

Applying these expressions, we can get

$$\pi(\lambda_{1,j}) = \frac{p_{1,j}}{p^*_{1,j}} \quad \text{and} \quad \pi(\lambda_{w1,j}) = \frac{p_{1,j}}{p^*_{w1,j}} . \tag{8}$$

Stagnation pressure in relative motion

$$p^*_{w1,j} = p^*_{1,j} \frac{\pi(\lambda_{1,j})}{\pi(\lambda_{w1,j})} . \tag{9}$$

Mass flow rate of cooling air

$$\dot{m}_{cool,j} = \Delta m_{cool} \dot{m}_{1,j} , \tag{10}$$

where Δm_{cool} is the relative cooling air mass rate at the exit.

Clearance losses [1]

$$\dot{m}_{cl,j} = \dot{m}_{1,j} \frac{\delta D}{h D_m} \left[1 + \frac{0.6}{\sin \beta_{2,j}} \left(\frac{l}{t} \right)^* \right] . \tag{11}$$

Parameters of gas at the exit

Mass flow rate

$$\dot{m}_{2,j} = \dot{m}_{1,j} + \dot{m}_{cool,j} + \dot{m}_{cl,j} . \tag{12}$$

Fuel-to-air ratio

$$f_2 = \frac{f_1}{1 + \left(\frac{\dot{m}_2}{\dot{m}_1} - 1 \right) (1 + f_1)} . \tag{13}$$

Stagnation enthalpy of the gas in relative motion, leaving the row of the blades

$$i^*_{w2,j} = i^*_{w1,j} \frac{\dot{m}_{1,j}}{\dot{m}_{2,j}} + c_p T^*_{cool,j} \frac{\dot{m}_{cool,j}}{\dot{m}_{2,j}} + c_p T^*_{r,j} \frac{\dot{m}_{r,j}}{\dot{m}_{2,j}} + \frac{u_2^2}{2} - \frac{\dot{m}_{1,j}}{\dot{m}_{2,j}} \frac{u_1^2}{2} , \tag{14}$$

where $T^*_{cool,j}, T^*_{cl,j}$ – stagnation temperature of cooling and leakage gases respectively.

From *Eq.* (14) the stagnation temperature of gases in relative motion, leaving the row

$$T^*_{w2,j} = \frac{i^*_{w2,j}}{c_p} . \tag{15}$$

From pressure ratio of the row of blades, the theoretical exit velocity in relative motion:

$$\pi(\lambda_{w2t,j}) = \pi(j) \longrightarrow \lambda_{w2t,j} = \left[\left(1 - \pi(j)^{\frac{\kappa-1}{\kappa}}\right)\frac{\kappa+1}{\kappa-1}\right]^{\frac{1}{2}} . \tag{16}$$

The maximum possible velocity in the slant [1]

$$\lambda_{w2t,\max} = \sqrt{\frac{\kappa+1}{\kappa-1}\left[1 - \frac{2}{\kappa+1}(\sin\beta_2)^{\frac{2(\kappa-1)}{\kappa+1}}\right]} . \tag{17}$$

If $\lambda_{w2t,j} > \lambda_{w2t,\max}$ then $\lambda_{w2t,j} = \lambda_{w2t,\max}$ else the theoretical exit velocity determined by *Eq.* (16).

In the throat if $\lambda_{w2t,j} \geq 1$ then $\lambda_{w0t,j} = 1$ else $\lambda_{w0t,j} = \lambda_{w2t,j}$.

The total enthalpy and the stagnation temperature

$$i^*_{w0} = i^*_{w1,j} + \frac{u^2_{2,j} - u^2_{1,j}}{2} , \quad T^*_{w0} = \frac{i^*_{w0}}{c_p} . \tag{18}$$

The losses of vanes and rotor blades can be divided into two parts:

- losses from the inlet till the throat characterised by velocity-loss factor ψ_{0j}, and
- losses from the throat till the exit (ψ_j).

The following losses are taken into account: profile losses, secondary flow loss and tip clearance loss. Friction losses [1]

$$\xi_{fr} = 0.02185(0.01065x^2 - 2.295x + 160.5)(0.1055y^2 - 0.3427y + 0.295) , \tag{19}$$

where

$$x = \begin{cases} \beta_1 + \beta_2 & \text{if} \quad \beta_1 + \beta_2 < 110^0 \\ 110^0 & \text{if} \quad \beta_1 + \beta_2 \geq 110^0 \end{cases} \qquad y = \begin{cases} \frac{\sin\beta_1}{\sin\beta_2} & \text{if} \quad \frac{\sin\beta_1}{\sin\beta_2} < 1.7 \\ 1.7 & \text{else} \end{cases} .$$

Trailing edge losses and losses due to Reynolds number [1]

$$\xi_{te} = 0.2\frac{\delta_k}{t\sin\beta_2} , \quad \Delta\xi_{Re} = \frac{2100}{Re} - 0.021 , \tag{20}$$

where $Re = \frac{\rho_2 w_2 l}{\mu}$, $\mu = (0.229x^3 - 1.333x^2 + 4.849x + \frac{0.275}{\alpha})10^{-5}$,

$$x = \frac{T}{10000} ; \quad \alpha \text{ is the air excess factor.}$$

Profile losses

$$\xi_p = \xi_{fr} + \xi_{te} + \Delta\xi_{Re} . \tag{21}$$

Increase in profile losses due to impact and secondary flow losses [1]

$$\Delta\xi_i = a(1-\xi_p)\left(\frac{\beta_{1g}-\beta_1}{\beta_1}\right)^2 , \quad \xi_s = 2\xi_p \frac{t\sin\beta_2}{h_2} . \tag{22}$$

Losses of mixing [1]

$$\xi_m = \frac{\dot{m}_{cool,j}}{\dot{m}_{1,j}}\left(1-\frac{c'_{1,j}}{c_{2,j}}\right)^2 , \tag{23}$$

where $c'_{1,j} = \frac{\dot{m}_{cool}}{\rho A_{cl,j}}$ and $A_{cl,j} = \frac{h_{cl,j}\delta_{cl,j}D_{m1,j}}{t_j}$. Velocity coefficient in the throat

$$\psi_{0,j} = \sqrt{1-(\xi_{fr}+\xi_s+\Delta\xi_{Re}+\Delta\xi_i)} , \tag{24}$$

and at the exit

$$\psi_j = \sqrt{1-(\xi_{fr}+\xi_s+\xi_k+\Delta\xi_{Re}+\Delta\xi_i+\xi_e)} . \tag{25}$$

The non-dimensional velocities

$$\lambda_{w0,j} = \lambda_{w0t,j}\psi_{0,j} , \quad \lambda_{w2,j} = \lambda_{w2t,j}\psi_j . \tag{26}$$

The pressure ratio can be determined by gas dynamic functions

$$\frac{p_{2,j}}{p^*_{w1,j}} = \pi(\lambda_{w2t,j}), \quad \frac{p_{2,j}}{p^*_{w2,j}} = \pi(\lambda_{w2,j}), \quad \frac{p_{0,j}}{p^*_{w0,j}} = \pi(\lambda_{w0t,j}), \quad \frac{p_{0,j}}{p^*_{w0,j}} = \pi(\lambda_{w0,j}).$$

Stagnation pressure in relative motion after the row of the blades and in throat

$$p^*_{w2,j} = p^*_{w1,j}\frac{\pi(\lambda_{w2t,j})}{\pi(\lambda_{w2,j})} , \quad p^*_{w0,j} = p^*_{w1,j}\frac{\pi(\lambda_{w0t,j})}{\pi(\lambda_{w0,j})} . \tag{27}$$

The mass flow rate of the row of blades

$$\dot{m}_{0,j} = \frac{p^*_{w0,j}A_{0,j}q(\lambda_{w0,j})}{\sqrt{T^*_{0,j}}}\sqrt{\frac{\kappa}{R}\left(\frac{2}{\kappa+1}\right)^{\frac{\kappa+1}{\kappa-1}}} . \tag{28}$$

Mass flow rate entering the row of blades

$$\dot{m}_{1,j} = \dot{m}_{,j} . \tag{29}$$

The exit mass flow rate

$$\dot{m}_{2,j} = \dot{m}_{1,j} + \dot{m}_{cool,j} - \dot{m}_{l,j} . \tag{30}$$

The relative exit velocity

$$w_{2,j} = \lambda_{w2,j}c_{cr} . \tag{31}$$

The exit Mach number

$$M_{2,j} = \lambda_{2,j}\sqrt{\frac{2}{(\kappa+1)\tau(\lambda_{2,j})}} \,. \tag{32}$$

Calculation of the flow deviation in the slant.

The exit angle [3]

$$\beta_{2,j} = \begin{cases} B_1 & \text{if} \quad M_{2,j} \le 0.5, \\ B_2 & \text{if} \quad 0.5 < M_{2,j} \le 1, \\ B_2 + \sin^{-1}\left(\frac{\sin\beta_{2g,j}}{q(\lambda_{w2,j})}\right) - \beta_{2g,j}. & \end{cases} \tag{33}$$

where

$$\begin{aligned} B_1 &= \left(1.1325\beta_{2g,j} - 1.925 + 4\frac{t}{e}\right)\frac{\pi}{180}\,, \\ B_2 &= \left[1 + 0.185\left(\frac{t}{e}\right)^2 + 0.03994\frac{t}{e}\right]\beta_{2g,j}^{rad}\,. \end{aligned}$$

The discharge absolute velocity from velocity diagram and the angle

$$c_{2,j} = \sqrt{w_{2,j}^2 + u_{2,j}^2 - 2c_{2,j}u_{2,j}\cos\beta_{1,j}}\,, \quad \alpha_{2,j} = \tan^{-1}\frac{w_{2,j}\sin\beta_{2,j}}{w_{2,j}\cos\beta_{2,j} - u_{2,j}}\,. \tag{34}$$

Stagnation enthalpy of the gas at the exit before mixing in the cooling air

$$i_{2,j}^* = i_{w2,j}^* - \frac{c_{2,j}^2 - w_{2,j}^2}{2}\,. \tag{35}$$

Non-dimensional discharge absolute velocity

$$\lambda_{2,j} = \frac{c_{2,j}}{c_{cr}}\,. \tag{36}$$

Static and stagnation pressure in absolute motion

$$p_{2,j} = p_{w1,j}^*\pi(\lambda_{w2t,j})\,, \quad p_{2,j}^* = p_{2,j}\pi(\lambda_{2,j})\,. \tag{37}$$

Static discharge temperature

$$T_{2,j} = T_{2,j}^*\tau(\lambda_{2,j})\,. \tag{38}$$

The absolute exit parameters of the row of blades will be the inlet parameters for the next row.

The set of non-linear equations will be composed from mass conservation equations for the rows of the blades.

$$\dot{m}_{1,j} + \dot{m}_{cool,j} + \dot{m}_{r,j} - \dot{m}_{2,j} = 0\,, \quad j = 1,\ldots,n\,. \tag{39}$$

The set of equations can be solved by numerical method.

1.2. Parameters of the Stages

After the calculation of a stator and a rotor row of the blades, it is necessary to find the parameters of the stage.

The actual power is determined as the power of the gas decreased by losses due to tip leakage and amount of heat rejected by cooling air

$$P_f = \dot{m}_{1,j-1}(i^*_{1,j-1} - i^*_{2,j})(1 - \Delta\eta_{leak}) - \dot{m}_{cool,j}c_p\Delta T_{cool,j} \,. \tag{40}$$

where decrease in efficiency due to leakage losses [1]

$$\Delta\eta_{leak} = \frac{\delta D''\rho''}{hD_m\rho_m}\left[1 + \frac{0.3}{\sin\beta_{2g}}\left(\frac{l}{t}\right)''\right] , \tag{41}$$

change in temperature of cooling air

$$\Delta T_{cool,j} = T''_{cool,j} - T'_{cool,j} \,. \tag{42}$$

Pressure ratio for the stage and exit stagnation temperature

$$\pi^*_{st} = \frac{p^*_{2j}}{p^*_{1,j-1}} , \quad T^*_{2s,j} = T^*_{1,j-1}\pi^{*\frac{\kappa-1}{\kappa}}_{st} \,. \tag{43}$$

Isentropic power for the stage

$$P_{s,st} = \dot{m}_{1,j}c_p(T^*_{1,j-1} - T^*_{2s,j}) \,. \tag{44}$$

Isentropic efficiency

$$\eta^{st}_s = \frac{P_{st}}{P_{s,st}} \,. \tag{45}$$

The exit stagnation enthalpy from energy balance

$$i^*_{2,j} = \frac{\dot{m}_{1,j-1}\left[i^*_{2,j} - (i^*_{1,j-1} - i^*_{2,j})\frac{\dot{m}_{leak}}{\dot{m}_{1,j-1}}\right] + \dot{m}_{cool,j}c_pT''_{cool,j}}{\dot{m}_{2,j}} \,. \tag{46}$$

1.3. Turbine Parameters

Stagnation temperature, non-dimensional velocity and stagnation pressure at the exit

$$T^*_2 = \frac{i^*_{2,j}}{c_p} , \quad \lambda_2 = \lambda_{2,j}\sqrt{\frac{T^*_{2,j}}{T^*_2}} ; \quad \dot{p}_2 = \frac{p_{2,j}}{\pi(\lambda_2)} \,. \tag{47}$$

Non-dimensional mass flow rate for the turbine

$$q(\lambda)_T = q(\lambda)_1 \,. \tag{48}$$

Actual power of the turbine

$$P_T = \sum_{i=1}^{z/2} P_{st_i} \, . \tag{49}$$

Stagnation pressure ratio for the turbine

$$\pi_T^* = \prod_{i=1}^{z/2} \pi_{st_i}^* \, . \tag{50}$$

Isentropic power of the turbine

$$P_{T_s} = \dot{m}_{1,2} c_p T_{1,1}^* \left[1 - (\pi_T^*)^{\frac{1-\kappa}{\kappa}}\right] \, . \tag{51}$$

Isentropic efficiency

$$\eta_{s_T} = \frac{P_T}{P_{T_s}} \, . \tag{52}$$

1.4. Calculation of $\lambda_u =$ const. Curves on Turbine Characteristics

The calculation concerning the given non-dimensional peripheral velocity

$$\lambda_u = \frac{u}{\sqrt{\frac{2\kappa}{\kappa+1} R T_{1,j}^*}} \tag{53}$$

can be continued by the variation of the pressure ratio of the first row of blades (by the reduction of the pressure ratio from $\pi(j) = 0.9$). In the course of calculations, one of the rows of blades will reach the critical operational mode (choking), and therefore its mass flow rate increase will stop and reaches its maximum value with the given λ_u, and further on the pressure distribution and the flow conditions will not change with the rows of blades preceding the latter one.

Subsequently, the variation of pressure ratio should be continued with the row of blades having reached the critical operational mode, and the equations associated with the former rows of blades should be separated from the system of equations for the mass flow rate conservation. Accordingly, the number of the independent variables $[\pi(j)]$ will also be reduced. The reduction of the pressure ratio should be continued up to the point when the critical operational mode occurs with another row of blades. In this case and afterwards, too, this procedure should be performed according to those described above until the choking occurs with the last row of blades, and the lower limit of pressure ratio range of the turbine to be calculated is reached. In the computing program, the search of the pressure ratio belonging to the critical operational mode is ensured by automatic step-halving of the pressure ratio in the neighbourhood of the critical operational mode. Then, after the separation of the choked part, the calculation can be resumed anew with the original step interval.

The simplified flow diagram of the calculations is shown on *Fig. 1.*

The temperature and constituent dependence of the specific heat and the adiabatic exponent, as well as the constituent dependence of the gas constant are taken into consideration with the help of the subroutine developed for this purpose.

The significance of the method elaborated for the computation of characteristics lies in the fact that it renders possible the direct determination of the characteristics of multi-stage turbines. There is no need for stage by stage calculation and then for the summation of characteristics – though a possibility is provided of displaying the data by stages, too. The Newton–Raphson method applied to the solution of the set of non-linear equations ensured a very rapid convergence.

Eqs. (39) and the relationships covered by those constitute the mathematical model of the turbine, which can be adapted directly on the models of the other units of gas turbine power plants.

2. Results of Turbine Characteristics' Calculations

Fig. 2 shows the maps of a single-stage and a double-stage gas turbine. On the vertical axis of the turbine characteristics built up of non-dimensional parameters, the non-dimensional mass flow rate developed in the minimum cross-section of the stator blades of the first stage and the turbine efficiency was represented, while the pressure ratio of the turbine was plotted on the horizontal axis. The non-dimensional peripheral velocity λ_u was a parameter. The constant sections $q(\lambda)$ seen on the characteristics show the fact that with the given pressure ratio, a choking occurred in a row of blades of the turbine.

In case the choking occurred for the first time in the row of stator blades of the first stage, then $q(\lambda) = 1$, while the straight sections $1 > q(\lambda) =$ constant seen on the double-stage characteristics (*Fig. 2b*) show that with a given value λ_u, a choking will occur first not in the nozzle of the first stage. As it is shown in the *Fig. 3* and *4* representing the variation of the mass flow rate and the pressure ratio as taking place in the rows of blades, this choking will occur in the third row of blades of the turbine examined. The diagrams on right side show the characteristics in case of decrease of the first stage nozzle exit angle.

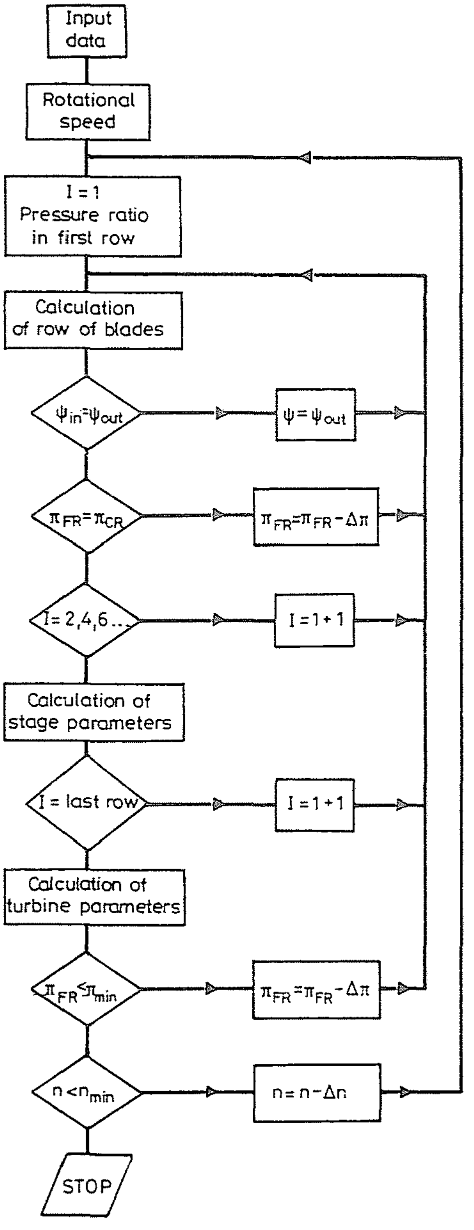

Fig. 1. Simplified flow diagram of the turbine model

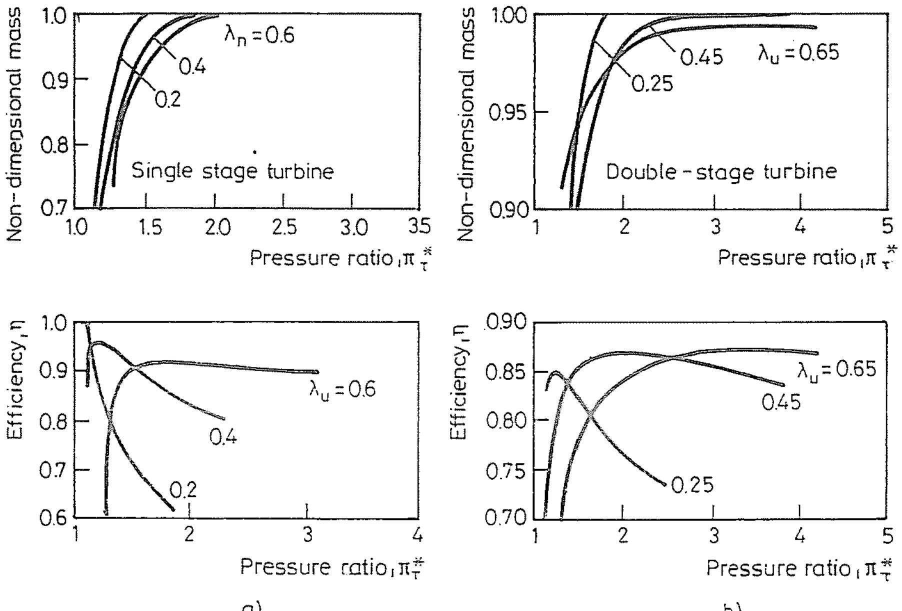

Fig. 2. Calculated turbine maps

3. Effect of Changes in Geometrical Parameters on Turbine Maps

The detailed turbine examinations were performed with the help of the turbine model for the two-stage gas generator turbine unit. In the course of examination, the inlet and outlet angles of blading by each row of blades, as well as the value of radial clearances of rotor blades were varied. The results of calculations are represented on *Figs. 5* and *6*. The dashed lines show a map of the turbine changed geometry.

The analysis of the calculation results as broken down to the level of the row of blades shows that the simulated variations will modify the turbine characteristics (*Figs. 5* and *6*). Depending on the character and measure of variations, the following characteristics will also be changed: the pressure ratio of the turbine as associated with the choking, the sequence of the choking the rows of blades, and as a consequence, the passing capacity of the turbine, as well as its efficiency.

Since the determination of the turbine characteristic of the models examined will take place on the basis of the geometrical characteristics of the turbine in question, this kind of examination will show the way to the correction of calculated characteristics.

From the detailed analysis of the results it can be established that the reduction in the outlet angle of the first-stage row of stator blades –

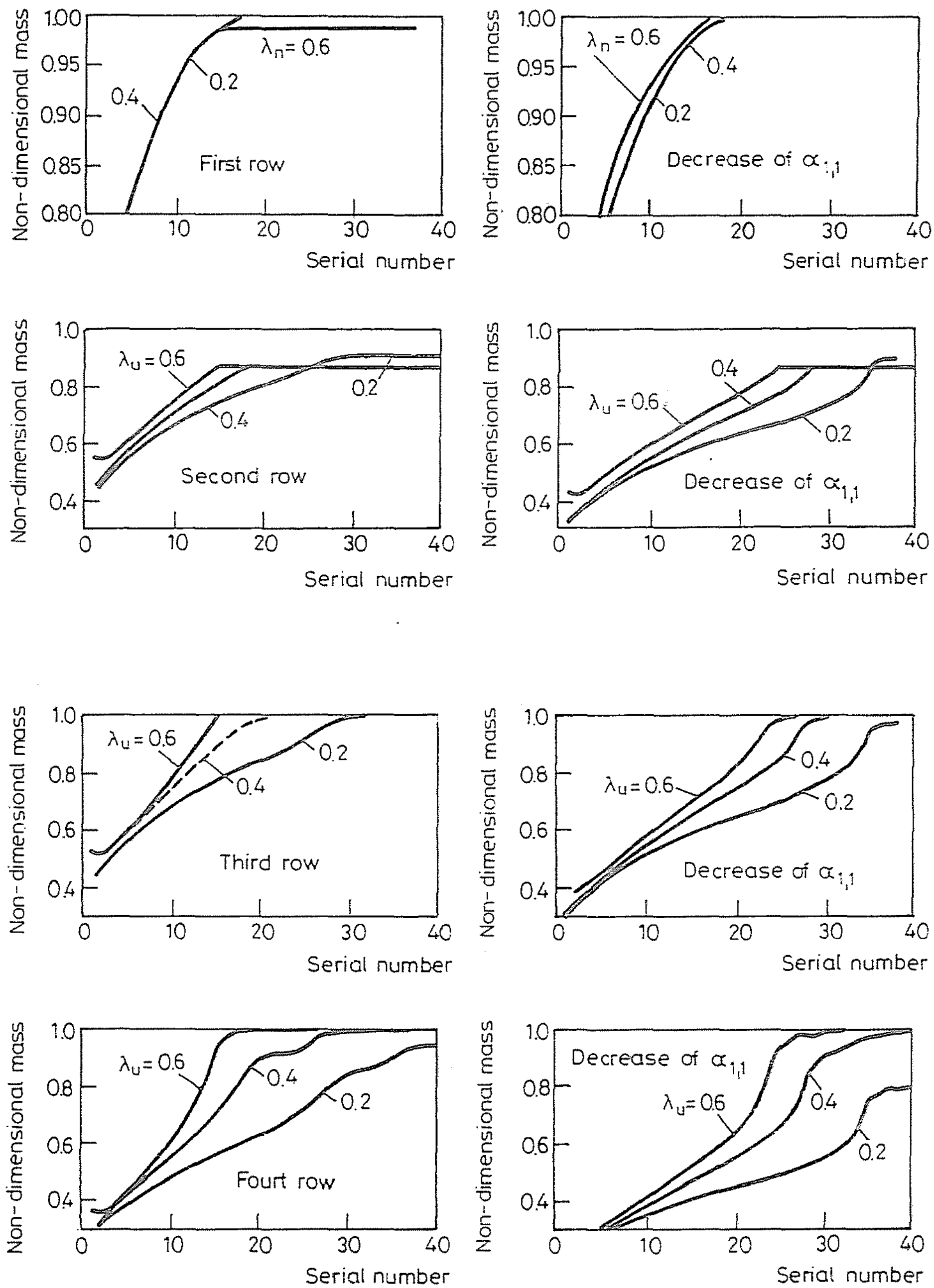

Fig. 3. Mass flow rate variations in the rows of blades

which, in turn, involves also the reduction in the cross-section – will shift the $\lambda_u =$ const. curves towards the lower pressure ratios of the turbine (*Fig. 5*). This result emanates from the fact that the reduction in cross-section will bring forward the chocking with the row of blade, i.e. the value of $q(\lambda)$ will increase. In this case the reduction of the outlet angle is performed with another row of blade subsequent to the first one, the mass flow rate curves will be shifted towards the higher pressure ratio of the turbine. These reductions in the cross-section will reduce the non-dimensional mass flow rate of the first row of blades, and this, in turn, will be reflected in the diagram.

The increase of radial clearances (*Fig. 6*) will bring no change in the path of the mass flow rate curves with the first or the second stages. The curves of efficiency will be shifted, in both cases, towards the reduction of them.

The highest non-dimensional mass flow rate will be obtained in case the choking occurs with the first-stage row of stator blades. In the case of an increase in the rpm, or more exactly in λ_u, the degree of reaction of the stage(s) will increase, and due to it, the non-dimensional mass flow rate of the stator blades row of the first stage will decrease, and the chocking can occur somewhere downstream, or, even with the row of rotor blades, respectively. (This process will last while β_1 is less than 90°, afterwards a reduction in the degree of reaction will occur.). The constant curves λ_u will be shifted towards the higher pressure ratios and downwards.

From the diagram a similar conclusion can be inferred concerning T_3^* – but due to the fact that it occurs in the denominator of λ_u with the opposite effect – the increase of the temperature will involve the decrease of the degree of reaction, and the non-dimensional mass flow rate will increase.

According to the examinations performed so far, the change in the inlet angle of the rotor blades will not modify considerably the non-dimensional mass flow rate. The reduction of the inlet angle will result in the widening to a small extent of the mass flow rate diagram, while its increase will narrow it. The values of efficiency will be modified due to the change in the angle of attack.

As a result of this examination, a possibility will be provided of designing an optimal turbine construction, as well as the correct determination of the character of turbine damage – in case of spacing out proper measuring points – when the turbine model of this level is integrated into the whole of the power-plant model.

4. Summary

The applied model is suitable – with the knowledge of the geometrical dimensions and the thermodynamic parameters – for the calculation of char-

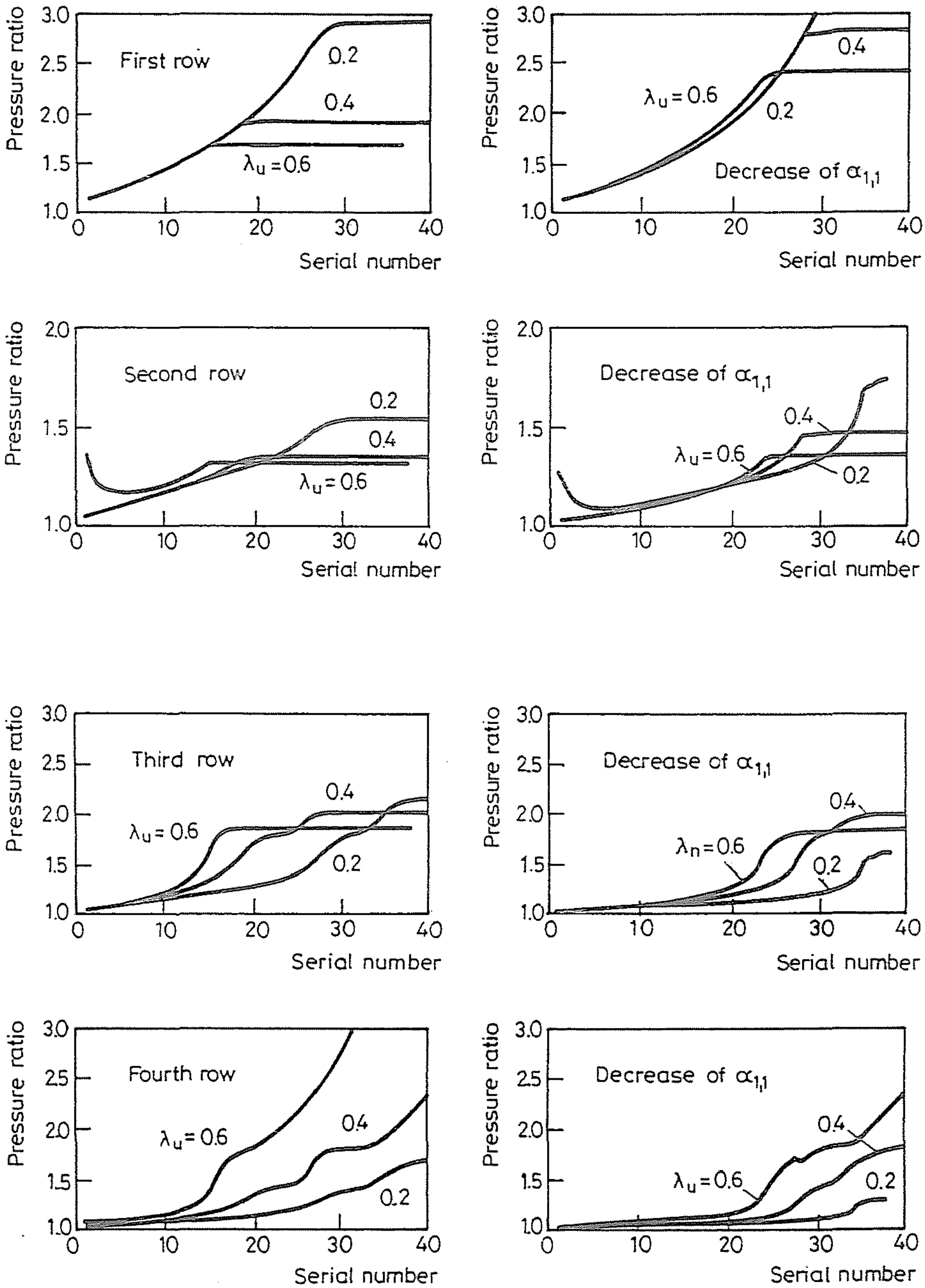

Fig. 4. Pressure ratio variations in the rows of blades

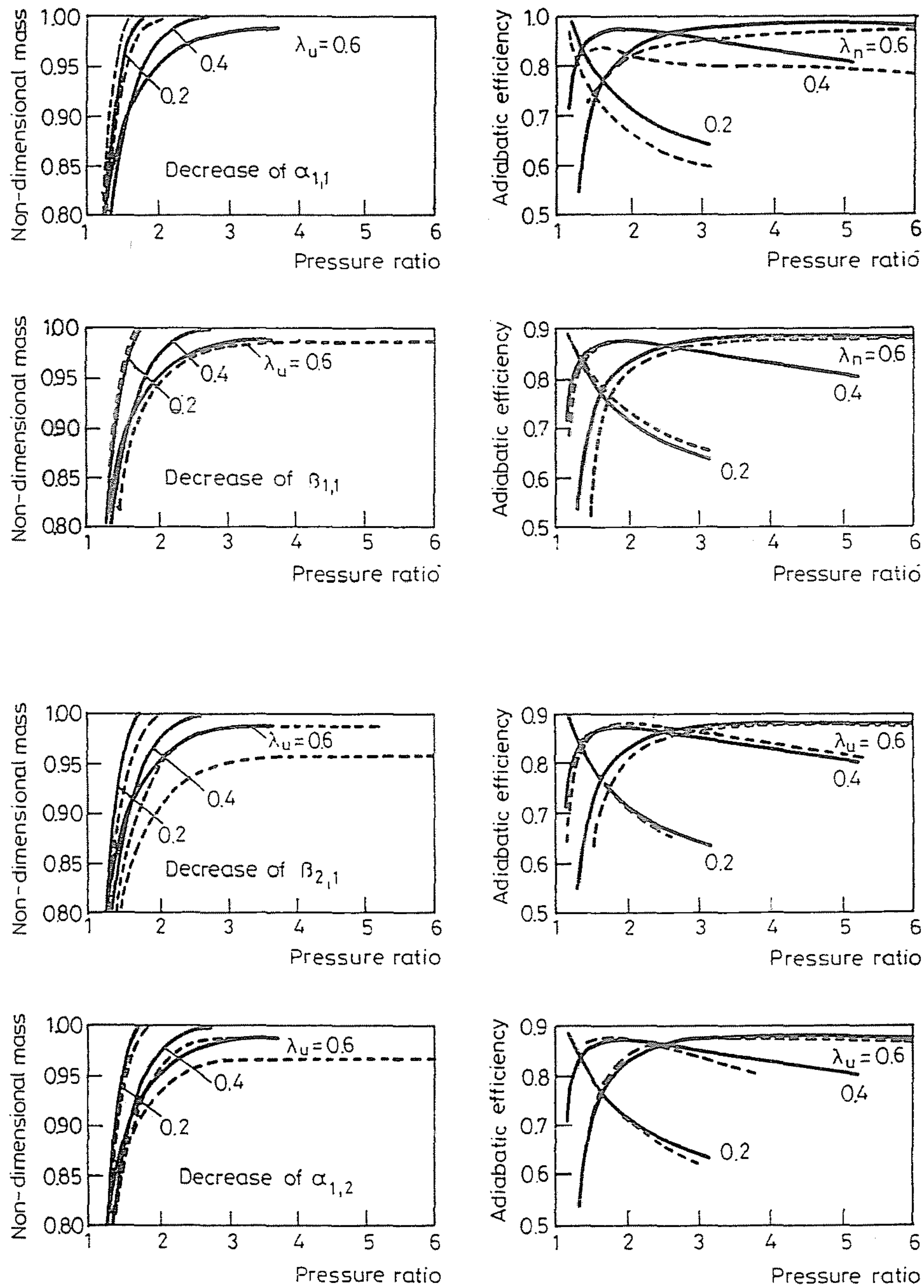

Fig. 5. Effect of changes in geometrical parameters on turbine map I

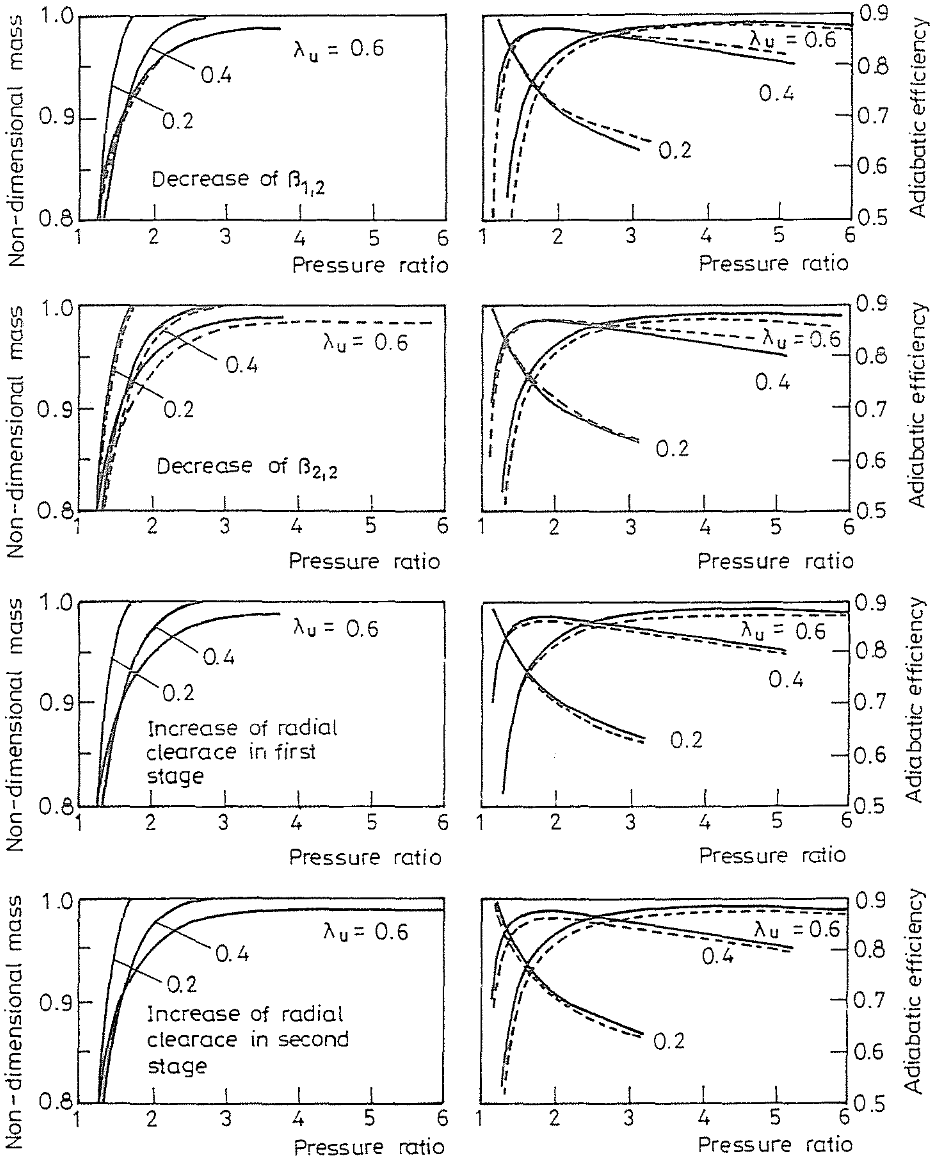

Fig. 6. Effect of change in geometrical parameters on turbine map II

acteristics and the examination of the processes taking place within the turbine in the course of both the design and operation. This model can be inserted – as a component model – into the mathematical model of the gas turbine power plants [4].

The examinations performed already, or to be performed later on, respectively, will provide information about the tendencies and possibilities of model adaptation.

The analysis of the calculation results as broken down to the level of the row of blades shows that the simulated variations will modify the turbine characteristics. Depending on the character and measure of variations, the following characteristics will also be changed: the pressure ratio of the turbine as associated with the choking, the sequence of the choking the rows of blades, and as a consequence, the passing capacity of the turbine, as well as its efficiency.

Acknowledgements

The author would like to acknowledge the support of Hungarian Oil Gas Indrusty Co., Hungarian Airlines MALEV and the Hungarian Scientific and Research Fund.

References

[1] ABIANC, B. H.: Teorija aviacionnüh gazovüh turbin, Masinosztroenie, Moscow, 1979.
[2] COHEN, H. – ROGERS, G. F. C. – SARAVANAMUTTOO, H. I. H.: Gas Turbine Theory, Longman, 1989.
[3] MUKHERJEE, D. K.: Berechnung der Druckziffer einer Turbine, *Z. Flugwiss.*, Vol. 16. 1968.
[4] SÁNTA, I.: Non-linear Mathematical Thermal Models of Gas Turbine Engines and Their Application in Operation, *ICAS Proceedings 1990*, Stockholm, Sweden, pp. 2264–2270.